Thermal, Crystallization, Mechanical, and Rheological Characteristics of Poly(trimethylene terephthalate)/Poly(ethylene terephthalate) Blends

PITT SUPAPHOL, NUJALEE DANGSEEYUN, PAKIN THANOMKIAT, MANIT NITHITANAKUL

The Petroleum and Petrochemical College, Chulalongkorn University, Soi Chula 12, Phyathai Road, Pathumwan, Bangkok 10330, Thailand

Received 30 April 2003; revised 27 September 2003; accepted 7 October 2003

ABSTRACT: Blends of poly(trimethylene terephthalate) (PTT) and poly(ethylene terephthalate) in the amorphous state were miscible in all of the blend compositions studied, as evidenced by a single, composition-dependent glass-transition temperature observed for each blend composition. The variation in the glass-transition temperature with the blend composition was well predicted by the Gordon–Taylor equation, with the fitting parameter being 0.91. The cold-crystallization (peak) temperature decreased with an increasing PTT content, whereas the melt-crystallization (peak) temperature decreased with an increasing amount of the minor component. The subsequent melting behavior after both cold and melt crystallizations exhibited melting point depression behavior in which the observed melting temperatures decreased with an increasing amount of the minor component of the blends. During crystallization, the pure components crystallized simultaneously just to form their own crystals. The blend having 50 wt % of PTT showed the lowest apparent degree of crystallinity and the lowest tensile-strength values. The steady shear viscosity values for the pure components and the blends decreased slightly with an increasing shear rate (within the shear rate range of 0.25–25 s^{-1}); those of the blends were lower than those of the pure components. © 2004 Wiley Periodicals, Inc. J Polym Sci Part B: Polym Phys 42: 676–686, 2004

Keywords: polymer blend; poly(trimethylene terephthalate); poly(ethylene terephthalate); miscibility

INTRODUCTION

Poly(ethylene terephthalate) (PET) and poly(buthylene terephthalate) (PBT) are linear aromatic polyesters that have been commercially available for quite some time. Both PET and PBT are versatile polymeric commodities. Poly(trimethylene terephthalate) (PTT) was recently introduced commercially by Shell Chemicals under the tradename Corterra. PTT has properties between those of PET and PBT, by taking an unusual combination of the outstanding properties of PET and processing characteristics of PBT. These characteristics make PTT highly suitable for uses in fiber, film, and engineering thermoplastics applications.

Polymer blending is an attractive alternative for producing new polymeric materials with desirable properties without having to synthesize a totally new material. Other advantages for polymer blending are versatility, simplicity, and inexpensiveness. Numerous published articles related to various aspects of binary blends of polyesters are available in the open literature. Some of these are, for example, blends of PET and PBT;[1–8] PBT and an amorphous co-polyester of cyclohexane di-

Correspondence to: P. Supaphol (E-mail: pitt.s@chula.ac.th)

Journal of Polymer Science: Part B: Polymer Physics, Vol. 42, 676–686 (2004)

nethanol, ethylene glycol, and terephthalic acid (PETG);[9] and PTT and poly(ether imide) (PEI).[10]

In PET/PBT blends, Escala and Stein[1] reported that the blends showed a single, composition-dependent glass-transition temperature (T_g) at all compositions suggesting that PET and PBT were miscible in the amorphous state. Similar results were also reported by others.[5,6] On the basis of various experimental techniques, Escala and Stein[1] reported that upon crystallization PET and PBT did not cocrystallize. Avramova[5] confirmed such findings and added that although each component formed its own crystalline phase upon crystallization, both components could crystallize concurrently at all compositions of the blends, and the presence of one crystalline phase did not deter or enhance the crystallization rates of the other.

In PBT/PETG blends, Nabi Saheb and Jog[9] reported that the blends exhibited a single, composition-dependent T_g at all compositions suggesting miscibility between PBT and PETG molecules in the amorphous state. The miscibility of PBT and PETG molecules was confirmed by the negative value of the interaction parameter. They also reported[9] that the blends exhibited composition-dependent, melting point depression, a direct result of the presence of PETG. In addition, an observed decrease in the crystallization rates for the blends as evidenced by an increase in the crystallization half-times was attributed to either an increase in the T_g or to a decrease in the ability of PBT molecules to mobilize because of the presence of PETG molecules.

Recently, Huang and Chang[10] investigated the miscibility, melting, and crystallization behavior of PTT/PEI blends. They observed[10] that the blends exhibited a single, composition-dependent T_g over the entire compositional range studied, indicating that the blends were fully miscible in the amorphous state. They also reported[10] that crystallization of PTT in the presence of PEI was either retarded (for blends having a PEI content of less than ca. 40 wt %) or fully inhibited (for blends having a PEI content of more than ca. 40%). The retardation in the crystallization rates for blends having a PET content of less than 40% was attributed to the decreased segmental diffusion of PTT molecules onto an existing growth face.

In this contribution, blends of PTT and PET were characterized for their thermal, crystallization, mechanical, and rheological behavior. The objectives for this work were: (1) to assess the miscibility of the blends in the amorphous state, (2) to investigate the effect of the blend composition on nonisothermal, cold and melt crystallizations and subsequent melting behavior, (3) to investigate the effect of blend composition on the mechanical property, (4) to assess the effect of blend composition on the apparent degree of crystallinity, and (5) to assess the effect of blend composition on the rheological behavior.

EXPERIMENTAL

Materials

PTT was supplied in pellet form by Shell Chemicals (Corterra CP509201 grade). The weight- and number-average molecular weights of this resin were about 78,100 and 34,700 Da, respectively. PET was supplied in pellet form by Indo PET (Thailand) (N1 grade). The weight- and number-average molecular weights of this resin were about 84,500 and 41,200 Da, respectively. The molecular weight characterization of these resins was carried out by size exclusion chromatography.

Sample Preparation

Both PTT and PET resins were dried in a vacuum oven at 140 °C for 5 h and then were premixed in a dry mixer to produce PTT/PET preblends of 10, 25, 40, 50, 60, 75, and 90% w/w of PTT, respectively. The preblends were then melt-mixed in a Collin ZK 25 self-wiping, corotating, twin-screw extruder, operating at a screw speed of 70 rpm and the die temperature of 280 °C. The extrudate was cooled in water and was pelletized with a Planetrol 075D2 pelletizer. The resulting blends are denoted xPTT/(1 − x)PET, where x is the weight percentage of PTT in the blends. Pure PTT, PBT, and their respective blends were then melt-pressed at 280 °C in a Wabash V50H compression press, with an applied pressure of 4.62 $\times 10^2$ MN · m^{-2} for 5 min before cooling to room temperature to produce films of approximately 200 μm in thickness.

Thermal Characterization

The decomposition temperatures (T_d's) for PTT, PET, and their blends were measured with a PerkinElmer Pyris Diamond thermogravimetric/differential thermal analyzer (TGA/DTA) within

the temperature range of 30–600 °C. The heating rate during thermal scanning was fixed at 10 °C · min^{-1} under nitrogen atmosphere. The temperatures at 10% weight loss (T_{10}) and at 50% weight loss (T_{50}) for each thermogram were reported.

A Mettler–Toledo DSC822^e differential scanning calorimeter (DSC) was used to record the nonisothermal cold- and melt-crystallization exotherms as well as the subsequent melting endotherms for PTT, PET, and their blends. Calibration for the temperature scale was carried out with a pure indium standard (T_m^o = 156.6 °C and ΔH_f^o = 28.5 J · g^{-1}) on every other run to ensure accuracy and reliability of the data obtained. To minimize thermal lag between the polymer sample and the DSC furnace, each sample holder was loaded with a disc-shaped sample weighing around 8.0 ± 0.5 mg, which was cut from the as-prepared films. Each sample was used only once, and all the runs were carried out under nitrogen atmosphere to prevent extensive thermal degradation.

The experiments started with heating PTT, PET, and their blends from 40 °C to a fusion temperature of 280 °C at a rate of 80 °C · min^{-1} for a melt-annealing period of 5 min to reset previous thermal histories, after which the samples were taken out and immediately quenched in liquid nitrogen to attain the completely amorphous state of the samples. To observe the nonisothermal cold-crystallization and subsequent melting behavior, each sample was reheated again with DSC from 25 to 280 °C at a rate of 10 °C · min^{-1}. After a melt-annealing period of 5 min at 280 °C, the sample was cooled to 30 °C at a cooling rate of 10 °C · min^{-1} to observe the nonisothermal melt-crystallization behavior and reheated again to 280 °C at a heating rate of 10 °C · min^{-1} to observe the subsequent melting behavior. These experiments allow one to obtain values for the T_g, the cold crystallization peak temperature (T_{cc}), the apparent cold-melting peak temperature (T_{cm}, subsequent melting after cold crystallization), the melt-crystallization peak temperature (T_{mc}), and the apparent melt-melting peak temperature (T_{mm}, subsequent melting after melt crystallization), respectively.

Crystal Structure and Apparent Degree of Crystallinity

A wide-angle X-ray diffraction (WAXD) technique was used to determine the crystal modification and apparent degree of crystallinity for melt-crystallized PTT, PET, and the blend samples that had been prepared in a PerkinElmer DSC-7 by cooling from 280 to 30 °C at a cooling rate of 10 °C · min^{-1}. Each sample, after being taken out of the DSC sample holder, was pasted onto a glass sample holder, with Vaseline as an adhesive. The WAXD intensity pattern for each sample was then collected on a Rigaku Rint 2000 X-ray diffractometer, equipped with a computerized data collection and analytical toolbox. The X-ray source (Cu Kα radiation, λ = 1.54 Å) was generated with an applied voltage of 40 kV and a filament current of 30 mA.

Mechanical Property Measurement

The tensile strengths of PTT, PET, and their blends were determined with an Instron 4206 universal testing machine, according to the ASTM D638-91 standard test method. The measurements were carried out with a 100-kN load cell at a 5 mm · min^{-1} crosshead speed. Dumbbell-shaped specimens were cut from the as-prepared sheets with a hydraulic cutting machine. The width of the specimen was about 13 mm and the gauge length was about 50 mm. The results were taken as an average from measurements of at least five specimens.

Shear Viscosity Measurements

Pure PTT, PET, and blend pellets were melt-pressed into circular disks of 1 mm in thickness and 25 mm in diameter. A Rheometric Scientific ARES RDA-II rheometer, with cone-and-plate configuration, was used to examine the steady and dynamic shear behavior of these materials. Before each measurement, the measuring chamber was heated to 260 °C, and the gap between the cone and the plate was set to 0.052 mm. For a steady-rate sweep test, the shear viscosity of the materials was determined as a function of shear rate. For a dynamic measurement, the strain values were chosen such that the experiment could be performed in the linear viscoelastic region.

RESULTS AND DISCUSSION

Thermal Stability

TGA is the most popular method used to characterize the thermal stability of polymers. Figure 1(a) shows the raw TGA results for PTT, PET, and their

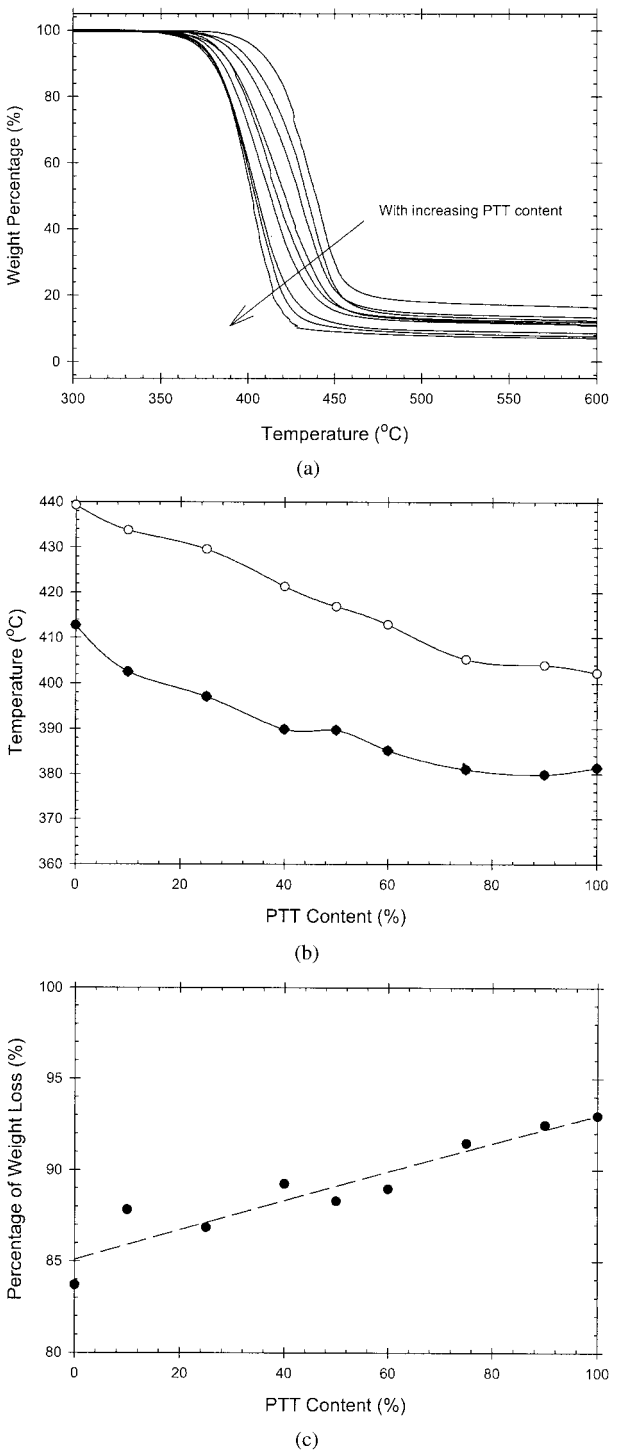

Figure 1. (a) Thermal-degradation curves in nitrogen atmosphere recorded with a heating rate of 10 °C · min^{-1} for PTT, PET, and their blends; (b) temperatures at (●) 10% and (○) 50% weight loss for PTT, PET, and their blends as a function of blend composition; and (c) ultimate percentage of weight loss for PTT, PET, and their blends as a function of blend composition.

blends. The temperature at 10% weight loss (T_{10}), taken as the onset of the degradation process, and the temperature at 50% weight loss (T_{50}) for PTT, PET, and their blends are shown in Figure 1(b). Obviously, pure PET was more thermally stable than pure PTT, and the thermal stability of the blend samples decreased monotonically with an increasing PTT content (or *vice versa*). This observation was postulated from the facts that the T_{10} values for PTT and PET were about 382 and 412 °C, respectively, and the T_{50} values for PTT and PET were about 402 and 440 °C, respectively, whereas both T_{10} and T_{50} values for the blends decreased monotonically from those of PET to approach those of PTT. It is also obvious from Figure 1(c) that the percentage of weight loss for PTT/PET blends increased monotonically from around 84% for pure PET to around 93% for pure PTT. The results confirmed that PTT, PET, and their blends were thermally stable within the temperature range used in all other measurements.

Miscibility of PTT/PET Blends

The presence of a single, composition-dependent T_g, located between those of the pure components, is indicative of miscibility of a given polymer pair in the amorphous phase. Figure 2(a) displays the DSC cold-crystallization and subsequent melting thermograms for quenched PTT, PET, and their blends recorded during heating with a heating rate of 10 °C · min^{-1}. It is apparent from Figure 2(a) that a single T_g value was observed in each thermogram and that the T_g value for the blend samples located between those of the pure components (i.e., $T_{g,PTT} \approx 44$ °C and $T_{g,PET} \approx 75$ °C) decreased with an increasing PTT content [see Fig. 2(b)]. The results clearly suggest that PTT and PET were fully miscible in the amorphous phase at all blend compositions. Another important observation that can be drawn from the raw data in Figure 2(a) is the specific heat-capacity jump (ΔC_p) at the glass-transition region. The ΔC_p values for PTT and PET were 0.28 and 0.36 $J \cdot g^{-1} \cdot K^{-1}$, and those for the blends containing 10, 25, 30, 50, 60, 75, and 90% of PTT were 0.33, 0.32, 0.26, 0.35, 0.36, 0.32, and 0.27 $J \cdot g^{-1} \cdot K^{-1}$, respectively.

A number of empirical models were proposed to predict the composition dependence of T_g for a pair of miscible polymer blends; some of these are the Gordon–Taylor,[11] Fox,[12] Couchman–Karasz,[13] and Utracki[14] equations. These equations predict a monotonic dependence of the T_g value on the blend

composition without any cusp in the predicted curve. Among these, the Fox equation has been widely used. In this model, the observed T_g value of the blends relates to the T_g values of the pure components 1 and 2 (i.e., T_{g1} and T_{g2}) and the blend composition according to the following equation:[12]

$$\frac{1}{T_g} = \frac{W_1}{T_{g1}} + \frac{W_2}{T_{g2}} \quad (1)$$

where W_1 and W_2 are the weight fractions (in the amorphous phase only) of components 1 and 2, respectively, and T_{g1} and T_{g2} are the T_g values of the pure components 1 and 2, respectively.

The Fox equation assumes random mixing between the two components, equal values of the ΔC_p in the glass-transition region between the two components (i.e., $\Delta C_{p1} = \Delta C_{p2}$), and no volume expansion between the two components during mixing. The dependence of the T_g value on the blend composition for PTT/PET blends is illustrated in Figure 2(b). The dotted line is the predicted composition dependence of the T_g value for PTT/PET blends according to the Fox equation. Apparently, the Fox equation underestimated the T_g value for the blends at all blend compositions. On the first approximation, the deviation of the T_g values from the Fox equation may be due to the fact that the ΔC_p of PTT and PET was not of equal values (0.28 vs 0.36 $J \cdot g^{-1} \cdot K^{-1}$), which evidently violates one of the assumptions used to attain the equation.

Another well-known equation used to predict the composition-dependent behavior of T_g for a pair of miscible polymer blends is the Gordon–Taylor equation,[11] which reads

$$T_g = \frac{W_1 T_{g1} + k W_2 T_{g2}}{W_1 + k W_2} \quad (2)$$

where k is an adjustable parameter. The solid line shown in Figure 2(b) is the predicted composition dependence of the T_g value for PTT/PET blends according to the Gordon–Taylor equation, with the fitting k parameter being 0.91. On the basis of the predicted curve and the data shown in Figure 2(b), agreement between the observed T_g values

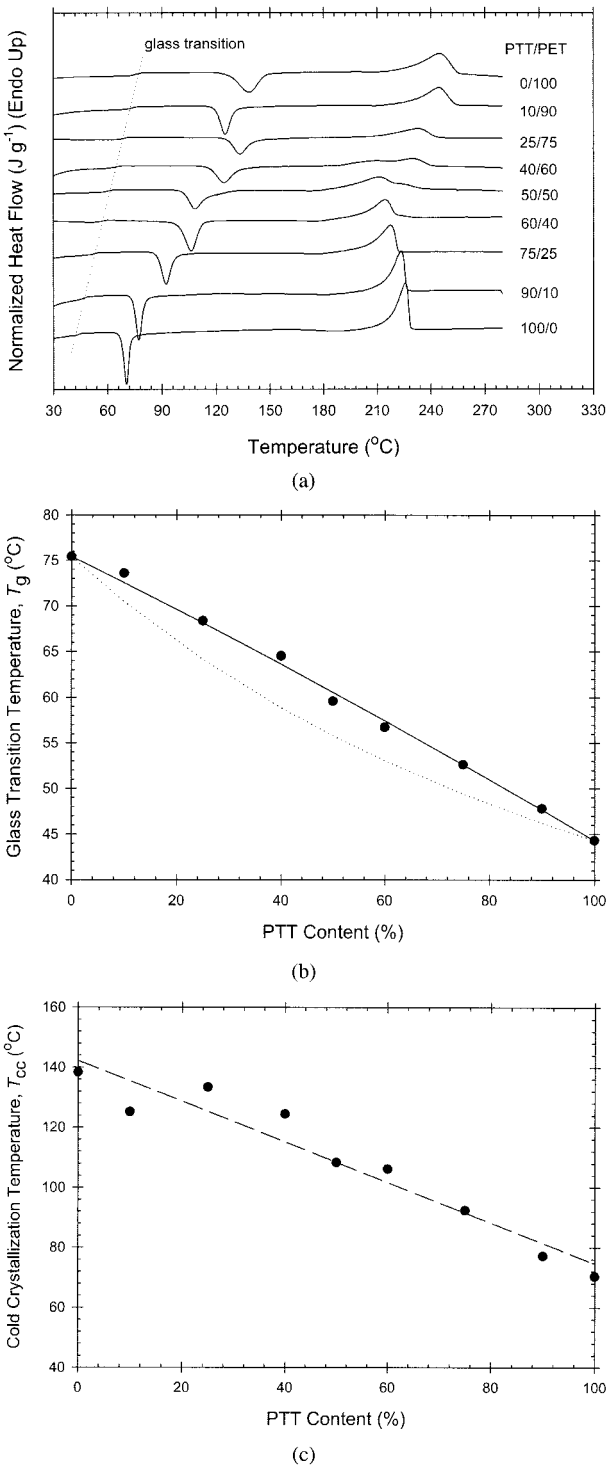

Figure 2. (a) DSC cold crystallization and subsequent melting thermograms for quenched PTT, PET, and blend samples recorded with a heating rate of 10 °C · min^{-1}. (b) Observed T_g for quenched PTT, PET, and their blends as a function of blend composition. The dotted line is the predicted T_g curve according to the Fox equation, and the solid line is the predicted T_g curve according to the Gordon–Taylor equation, with the fitting parameter k of 0.91. (c) T_{cc} for quenched PTT, PET, and their blends as a function of blend composition.

and the prediction by the Gordon–Taylor equation was obtained at all blend compositions.

Crystallization Behavior

According to Figure 2(a), the cold-crystallization (peak) temperature (T_{cc}) for PTT was observed around 70 °C, whereas that of PET was observed around 138 °C, suggesting that PTT was more crystallizable than PET. The observed T_{cc} values for PTT/PET blends [taken from the thermograms shown in Fig. 2(a)] were plotted against the blend composition in Figure 2(c). Obviously, a single, composition-dependent T_{cc} value was observed for each blend; the observed T_{cc} value decreased hypothetically linearly from around 138 to 70 °C with an increasing PTT content (with an exception to the observed T_{cc} value for the 10PTT/90PET blend that was lower than those values for the pure PET and 25PTT/75PET blends). The results suggested that both PTT and PET components in the blends crystallized simultaneously and that the commingled addition of the more crystallizable PTT molecules to PET helped promote the crystallizability of the blends. The explanation for the peculiar result observed for the 10PTT/90PET blend is not yet available, and it should be a subject for further investigation.

Figure 3(a) shows the DSC melt-crystallization exotherms for PTT, PET, and their blends recorded during cooling at a cooling rate of 10 °C · min^{-1}. According to Figure 3(a), the melt-crystallization (peak) temperature (T_{mc}) for PTT was observed around 180 °C, whereas that of PET was observed around 204 °C, suggesting, again, that PTT was more crystallizable than PET. The observed T_{mc} values for PTT/PET blends [taken from the exotherms shown in Fig. 3(a)] were plotted as a function of the blend composition in Figure 3(b). Similar to the case of cold crystallization, a single, composition-dependent T_{mc} value was observed for each blend, with the observed T_{mc} value decreasing monotonically with an increasing amount of the minor component of the blends. The results suggested that both PTT and PET components in the blends crystallized simultaneously and that an increase in the amount of the minor phase retarded the crystallizability of the blends, or, in other words, the crystallization ability of the major component in the blends decreased with an increasing amount of the minor component. Interestingly, the facts that the 40PTT/60PET blend exhibited the lowest T_{mc} value and that its crystallization exotherm was almost unobservable under the cooling rate examined suggested that crystallization was almost inhibited for this particular blend.

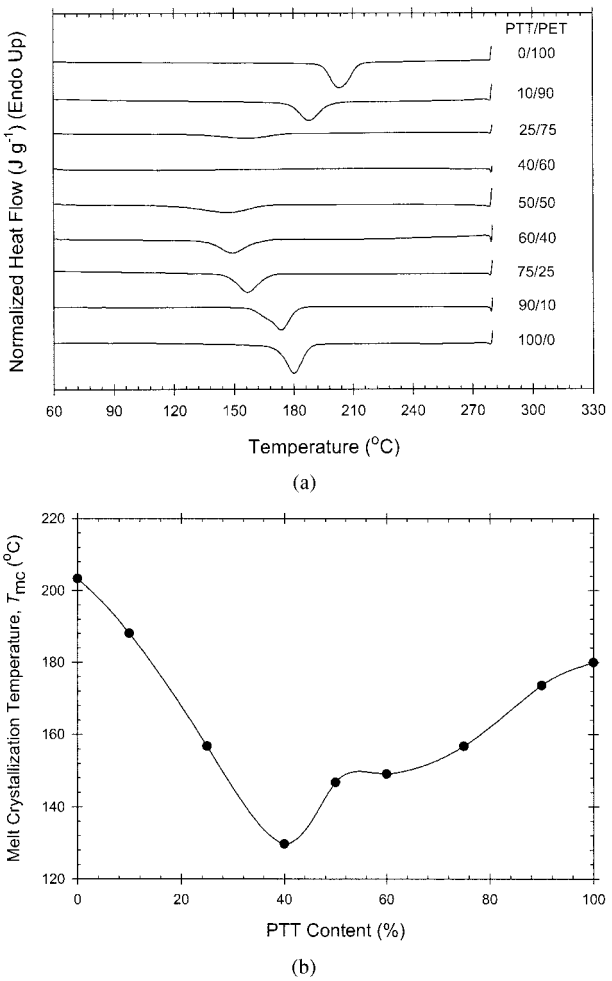

Figure 3. (a) DSC melt-crystallization thermograms for PTT, PET and their blends recorded with a cooling rate of 10 °C · min^{-1} and (b) T_{mc} for PTT, PET, and their blends as a function of blend composition.

Crystal Structure and Apparent Degree of Crystallinity

The crystal structures and the apparent degrees of crystallinity for PTT, PET, and their blends (nonisothermally crystallized from the molten state at a cooling rate of 10 °C · min^{-1}) were observed with WAXD, of which the results are depicted in Figure 4(a). The characteristic X-ray peaks for PTT were observed at the scattering angles 2θ of about 15.3, 16.8, 19.4, 21.7, 23.6, 24.6, and 27.3°, corresponding to the reflection planes of (010), (0$\bar{1}$2), (012), (10$\bar{2}$), (102), (1$\bar{1}$3), and (10$\bar{4}$),

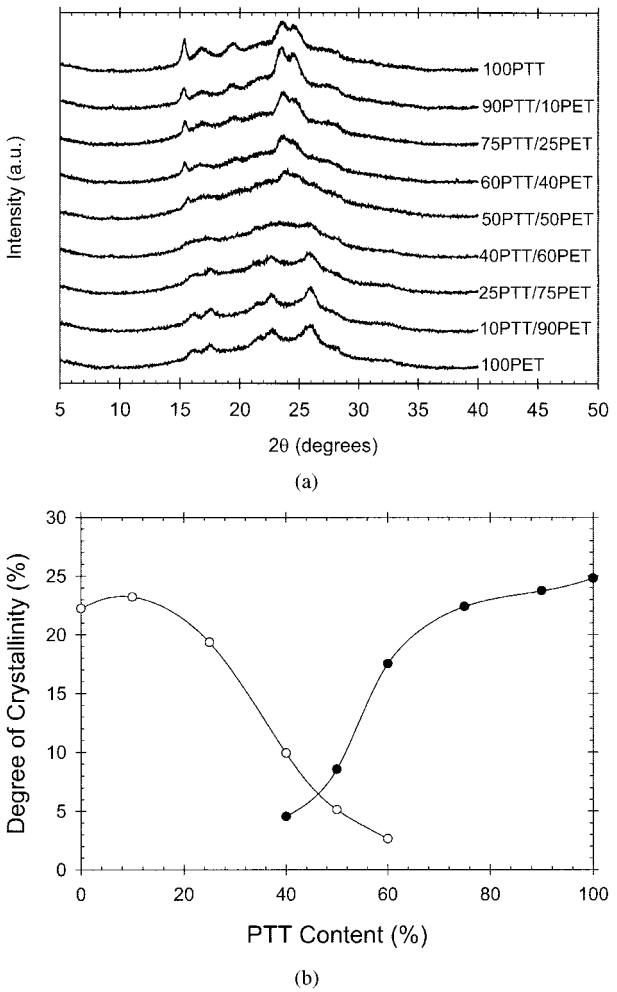

Figure 4. (a) WAXD patterns for PTT, PET, and their blends after nonisothermal crystallization from the molten state in the DSC cell at a cooling rate of 10 °C · min^{-1} and (b) apparent degree of crystallinity for (●) PTT and (○) PET components for both pure and blend samples as a function of blend composition.

respectively.[15] In the case of PET, the characteristic X-ray peaks were observed at the scattering angles (2θ) of about 16.1, 17.5, 21.6, 22.8, 25.9, 28.1, and 32.6°, corresponding to the reflection planes of $(0\bar{1}1)$, (010), $(\bar{1}11)$, $(1\bar{1}0)$, (100), $(1\bar{1}1)$, and (101), respectively.[16] Both PTT and PET crystallized into triclinic crystal structure, with the unit cell parameters for PTT being a = 4.64 Å, b = 6.27 Å, c = 18.64 Å, α = 98°, β = 90°, and γ = 111°[17] and for PET being a = 4.56 Å, b = 5.94 Å, c = 10.75 Å, α = 98.5°, β = 118°, and γ = 112°,[16] respectively.

The characteristic X-ray peaks for all the samples studied [taken from the diffractograms shown in Fig. 4(a)] are summarized in Table 1. Apparently, apart from those of the pure components, no new peaks were observed in the diffraction patterns of the PTT/PBT blend samples, indicating that the PTT and PBT components in the blend crystallized separately to form its own crystallites, even though it was shown that both components crystallized simultaneously during nonisothermal crystallization from both the glassy and the molten states.

Another important observation that was obtained from the WAXD patterns is the apparent degree of crystallinity (χ_c^{WAXD}). The χ_c^{WAXD} can be calculated from the ratio of the integrated intensities under the crystalline peaks (A_c's) to the integrated total intensities (A_t's) (i.e., $A_t = A_c + A_a$, where A_a is the integrated intensities under the amorphous halo). According to this procedure, the χ_c^{WAXD} values for the PTT and PET samples prepared in the condition prescribed in this work were around 25 and 22%, respectively. The value obtained for PTT agreed with the values reported by Chuah et al.[18] for melt-crystallized PTT samples of around 15–30%. The obtained χ_c^{WAXD} val-

Table 1. Characteristic X-ray Peaks and the Total Degree of Crystallinity of PTT, PET, and Blends

Blend Composition	Characteristic X-ray Peaks (2θ)														Degree of Crystallinity
PET	—	16.1	—	17.5	—	21.6	—	22.8	—	—	25.9	—	28.1	32.6	22
10PTT/90PET	—	16.1	—	17.6	—	21.5	—	22.7	—	—	25.9	—	27.8	32.5	23
25PTT/75PET	—	16.2	—	17.5	—	21.4	—	22.7	—	—	25.9	—	27.9	32.4	19
40PTT/60PET	15.5	16.2	—	17.5	—	21.6	—	22.7	23.4	24.5	25.8	—	28.0	32.7	15
50PTT/50PET	15.7	—	16.9	17.3	19.7	21.6	—	22.6	23.9	24.8	26.2	27.6	—	32.9	14
60PTT/40PET	15.4	—	16.7	17.4	19.8	—	21.8	—	23.6	24.6	26.0	27.2	—	32.7	20
75PTT/25PET	15.4	—	16.9	—	19.5	—	21.7	—	23.6	24.7	—	27.5	—	—	22
90PTT/10PET	15.3	—	16.8	—	19.3	—	21.6	—	23.4	24.6	—	27.6	—	—	24
PTT	15.3	—	16.8	—	19.4	—	21.7	—	23.6	24.6	—	27.3	—	—	25

ues of each component for the PTT/PET blends [calculated from the diffractograms shown in Fig. 4(a)] were plotted as a function of the blend composition in Figure 4(b), whereas the total χ_c^{WAXD} values are summarized in Table 1.

According to Figure 4(b), the χ_c^{WAXD} values for both PTT and PET components in the blends decreased monotonically with an increasing content of the other component. According to Table 1, the total χ_c^{WAXD} value for the blends decreased from that of PET (i.e., 22%) with an increasing PTT content, reaching minimum values of around 14–15% for 40PTT/60PET and 50PTT/50PET blends, and, finally, increasing with a further increase in the PTT content until approaching that of PTT (i.e., 25%). The total χ_c^{WAXD} values for the PET-rich blends were lower than those for the PTT-rich blend—a direct result of the higher crystallizability of PTT-rich blends. Similar behavior was also reported for blends of poly(ethylene naphthalate) and poly(buthylene naphthalate).[19]

Melting Behavior

The subsequent melting thermograms for PTT, PET, and blend samples after cold crystallization are shown in Figure 2(a). The thermograms for both PTT and PET samples exhibited single melting endothermic peaks, with the observed T_{cm}'s observed around 226 and 245 °C, respectively. PTT/PET blends having PTT contents of 10, 75, and 90% exhibited one endothermic peak, whereas those having PTT contents of 25, 40, 50, and 60% exhibited double-melting endothermic peaks. Figure 5 summarizes the observed T_{cm} values for PTT, PET, and blend samples as a function of the PTT content. According to Figure 5, the observed T_{cm} value for the major component of the blends decreased with an increasing amount of the minor component. The results obtained suggested that the subsequent melting temperature after cold crystallization is mainly dictated by the content of the minor component in the blends rather than by the crystallization temperature, which is in contradiction to the general knowledge for melt crystallization.

In blends of low contents of the minor component (e.g., 10PTT/90PET, 25PTT/75PET, 60PTT/40PET, 75PTT/25PET, and 90PTT/10PET blends), observation of the single melting endotherm suggested that even though the minor phase could form its own crystalline phase during cold crystallization, the amount of the crystalline phase of the minor component, as compared with the amount of the crystalline phase of the minor component formed, may not be enough to show its own distinctive melting endotherm during subsequent melting in DSC. In blends of intermediate contents of the minor component (e.g., 40PTT/60PET and 50PTT/50PET blends), observation of the double-melting endotherms confirmed that each component of the binary blends forms its own crystalline phase during cold crystallization.

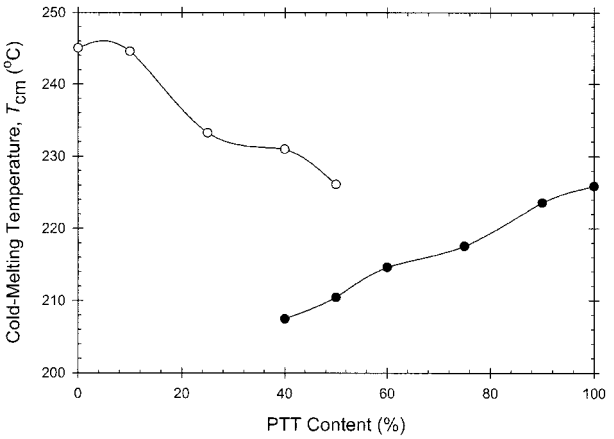

Figure 5. T_{cm} characterizing the melting of (●) PTT and/or (○) PET crystallites for quenched PTT, PET, and blend samples (after cold-crystallization process) as a function of blend composition.

Figure 6(a) shows the subsequent melting thermograms for PTT, PET, and the blend samples after melt crystallization. The melting behavior of PTT and PTT-rich blends exhibited the usually observed melting-recrystallization-remelting phenomenon, as evidenced from a small exothermic peak immediately before the remelting peak. Interestingly, the subsequent melting thermogram for the 40PTT/60PET blend apparently exhibited a cold-crystallization exotherm, suggesting that this particular blend was not able to crystallize during cooling at 10 °C · min^{-1} [see also the melt-crystallization thermogram for this particular blend in Fig. 3(a)]. Regardless of the multiple-melting phenomenon, the observed T_{mm}'s are summarized in Figure 6(b).

According to Figure 6(b), the observed T_{mm} values for PTT and PET were observed around 226 and 244 °C, respectively, which agreed with the T_{cm} values observed, and both PET- and PTT-rich blends exhibited the melting point depression phenomenon in that the observed T_{mm} value of the blend decreased with an increasing content of the minor component. The blend having equal contents of both PTT and PET exhibited the low-

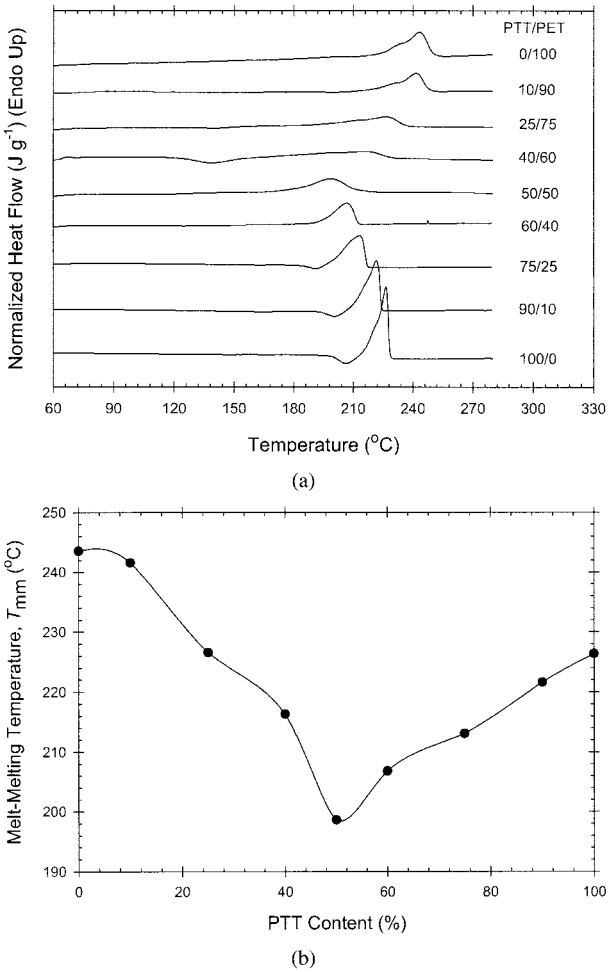

Figure 6. (a) Subsequent melting thermograms for PTT, PET, and blend samples after melt crystallization at a cooling rate of 10 °C · min^{-1}. The thermograms were recorded with a heating rate of 10 °C · min^{-1}. (b) Observed T_{mm} characterizing the melting of PTT, PET, and blend samples (after the melt-crystallization process) as a function of blend composition.

est observed T_{mm} value. The melting point depression can be used to study interactions between polymer molecules of two different species when one of the components in the miscible blends is partially crystalline. Because of the lowered chemical potentials of the molecules in the blends as compared with those of the pure state, the temperature at which the crystals of one component are in equilibrium with the miscible amorphous phase consisting of both components will be lower, leading to the occurrence of the melting point depression phenomenon.[20] The melting point depression phenomenon for both of the pure components in the miscible blends of PET and PBT was also observed.[5,21]

Mechanical Property

Figure 7 shows the tensile strengths of melt-crystallized PTT, PET, and the blend samples measured according to the ASTM D638-91 standard test method as a function of the PTT content. The tensile strength value for PTT was 58.3 MPa, which was lower than the value of 67.6 MPa reported by Chuah et al.,[18] whereas the value for PET was 73.8 MPa, which agreed with the value of 72.5 MPa reported by Chuah et al.[18] According to Figure 7, the lowest tensile strength was observed for the 50PTT/50PET blend. Because the observed T_{mc}, T_{mm}, and total χ_c^{WAXD} values for 50PTT/50PET blend were among the lowest, it is logical to postulate that the lowest amount of crystalline phase attributes a great deal to the lowest tensile strength value observed for this particular blend. Interestingly, the tensile strength value for both PET- and PTT-rich blends increased with an increasing amount of the minor component.

Melt Rheology

Figure 8 illustrates the steady shear viscosity (η) measured at 260 °C for PTT, PET, and their blends as a function of shear rate. Within the shear-rate range studied (i.e., 0.25–25 s^{-1}), the shear viscosity for these samples decreased very slightly with an increasing shear rate, suggesting a slight shear-thinning behavior. Chuah et al.[18] found that molten PTT behaved like a Newtonian fluid at low shear rates and like a shear-thinning fluid at shear rates greater than 1000 s^{-1}. The zero shear viscosity values (η_0's) for PET and PTT

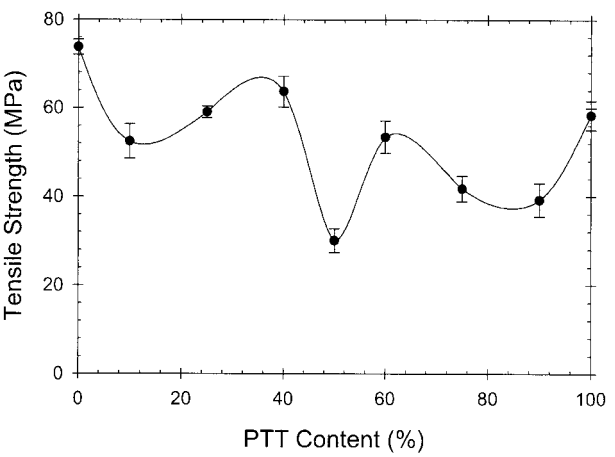

Figure 7. Tensile strength for PTT, PET, and their blends as a function of blend composition.

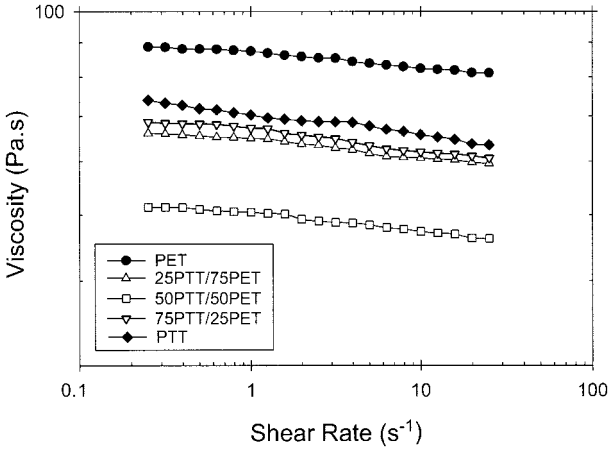

Figure 8. η measured at 260 °C for PTT, PET, and their blends as a function of shear rate.

were around 89 and 74 Pa · s. The reason for the shear viscosity of PET being greater than PTT may be attributed to the lower difference between the testing temperature and the observed T_{mm} value of PET than that of PTT (i.e., 16 °C for PET and 34 °C for PTT). For a given shear rate, the η of PET was the highest, followed by those values of PTT, 75PTT/25PET, 25PTT/75PET, and 50PTT/50PET. The η_0 values for 75PTT/25PET, 25PTT/75PET, and 50PTT/50PET blends were around 68, 66, and 51 Pa · s, respectively. With the observed T_{mm} values for these blends being around 214, 226, and 198 °C, the reason for the shear viscosity values of the blends being lower than those of the pure components may also be attributed to the larger difference between the testing temperature and the observed T_{mm} value of the blends as compared with those of the pure components (i.e., 46 °C for 75PTT/25PET, 34 °C for 25PTT/75PET, and 62 °C for 50PTT/50PET vs 16 °C for PET and 34 °C for PTT). The correlation between the largest difference between the testing temperature and the observed T_{mm} value and the lowest shear viscosity values for the 50PTT/50PET blend was apparent.

The dynamic complex viscosities (η^*'s) for PTT, PET, and blend samples as a function of frequency were measured at 260 °C, but the results are not shown. All of the observed η^* values for these samples were almost independent of the frequency used and ranked in the following order: PET > 25PTT/75PET ≈ 50PTT/50PET > 75PTT/25PET > PTT. Figure 9 shows the η^* value for PTT, PET, and their blends as a function of the blend composition for three different frequencies.

In polymer blends, the compositional dependence of a viscoelastic function gives much information about the degree of miscibility between the two constituents. The viscosity function usually follows the log-additivity rule, which states that

$$\log F_b = \phi_m \log F_m + \phi_d \log F_d \quad (3)$$

where F is a given viscoelastic function; ϕ is a volume fraction; and subscripts b, m, and d indicate the values for blend, the matrix, and dispersed phase, respectively.[22]

The miscibility of the polymer blends can be roughly determined from the deviation of the viscoelastic function from that predicted by the log-additivity rule mentioned previously. Three types of deviation can occur: (1) positive, (2) negative, and (3) positive/negative. For immiscible polymer blends, the positive deviation is expected, and for miscible blends the negative deviation should result. According to Figure 9, the blends having PTT contents of 25 and 75% showed strong negative deviation from the prediction by the log-additivity rule for all of the frequencies reported, suggesting total miscibility of the two constituents, whereas the blend having a PTT content of 50% showed slightly negative deviation from the prediction, suggesting the highest tendency for phase separation of the two components.

CONCLUSIONS

Blends of PTT and PET exhibited a single, composition-dependent T_g at all blend compositions

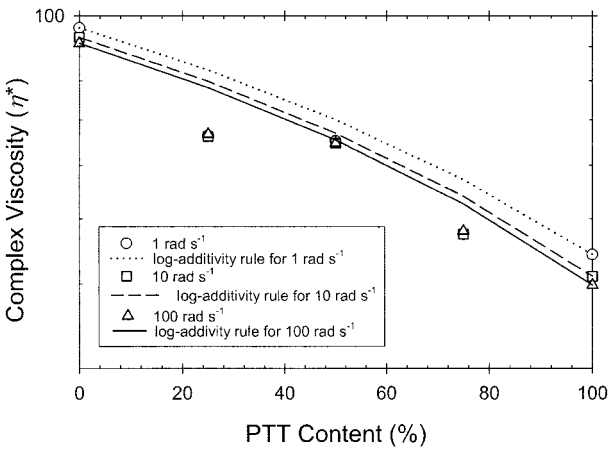

Figure 9. η^* measured at 260 °C for PTT, PET, and their blends as a function of blend composition for three different frequencies.

studied, indicating that both components were miscible in the amorphous phase. The observed T_g decreased monotonically with an increasing PTT content and was fit well to the Gordon–Taylor equation, with the fitting parameter k being about 0.91. The cold-crystallization (peak) temperature decreased with an increasing PTT content, whereas the melt-crystallization (peak) temperature decreased with an increasing amount of the minor component in the blends. The subsequent melting behavior for these blends after both cold and melt crystallization showed melting point depression behavior, in that the observed melting (peak) temperatures for the major component in the blends decreased with an increasing amount of the minor component. Both the crystallization behavior and WAXD studies suggested that both of the pure components in the blends crystallized simultaneously to form their own crystalline entities. The total apparent degree of crystallinity of the blends decreased from those of the pure components with an increasing content of the minor component, with the lowest values observed for the blends having PTT contents of 40–50%. The lowest apparent degree of crystallinity observed for the blend having a PTT content of 50% may be responsible for the lowest tensile strength observed. The steady shear viscosities for the pure components and the blends showed a slight shear-thinning behavior (within the shear-rate range of 0.25–25 s^{-1}), and the steady shear viscosities for the blends were systematically lower than those of the pure components, a direct result of the larger difference between the testing temperature and the observed melting temperature of the blends. Evaluation of the compositional dependence of the complex viscosities of the blends at three different frequencies according to the log-additivity rule suggested that the blends having PTT contents of 25 and 75% showed total miscibility of the two components, whereas the blend having a PTT content of 50% showed the highest tendency for phase separation.

The authors thank Hoe H. Chuah and his coworkers of Shell Chemical Co. for supplying PTT and for their kind assistance with the molecular weight measurements on all of the polyester resins received, Indo PET (Thailand), Ltd. for supplying the PET resin, and Anuvat Sirivat of Petroleum and Petrochemical College for his technical knowledge on the rheological measurements. P. Supaphol acknowledges a grant provided by Chulalongkorn University through the Development Grants for New Faculty/Researchers. Partial support from the Petroleum and Petrochemical Technology Consortium and Petroleum and Petrochemical College is noted.

REFERENCES AND NOTES

1. Escala, A.; Stein, R. S. Adv Chem Ser 1979, 176, 455.
2. Mishra, S. P.; Deopura, B. L. Polym Commun 1985, 26, 5.
3. Mishra, S. P.; Deopura, B. L. J Appl Polym Sci 1987, 33, 759.
4. Avramov, I.; Avramova, N. J Macromol Sci Phys 1991, 30, 335.
5. Avramova, N. Polymer 1995, 36, 801.
6. Shonaike, G. O. Eur Polym J 1992, 28, 777.
7. Yu, Y.; Choi, K. J. Polym Eng Sci 1997, 37, 91.
8. Lee, S. S.; Kim, J.; Park, M.; Lim, S.; Chul, R. C. J Polym Sci Part B: Polym Phys 2001, 39, 2589.
9. Nabi Saheb, D.; Jog, J. P. J Polym Sci Part B: Polym Phys 1999, 37, 2439.
10. Huang, J. M.; Chang, F. C. J Appl Polym Sci 2002, 84, 850.
11. Gordon, M.; Taylor, J. S. J Appl Chem 1952, 2, 493.
12. Fox, T. G. Bull Am Phys Soc 1956, 2, 123.
13. Couchman, P. R.; Karasz, F. E. Macromolecules 1978, 11, 117.
14. Utracki, L. A. Adv Polym Technol 1985, 5, 33.
15. Wang, B.; Li, Y. C.; Hanzlicek, J.; Cheng, S. Z. D.; Gail, P. H.; Grebowicz, J.; Ho, R. M. Polymer 2001, 42, 7171.
16. Wang, Z. G.; Hsiao, B. S.; Fu, B. X.; Lui, L.; Yeh, F.; Sauer, B. B.; Chang, H.; Schultz, J. M. Polymer 2000, 41, 1791.
17. Desborough, I. J.; Hall, I. H.; Neisser, J. Z. Polymer 1979, 20, 419.
18. Chuah, H. In Modern Polyester; Scheirs, J.; Long, T., Eds.; Wiley: Hoboken, NJ, 2003, Chapter 11.
19. Yun, K. H.; Lee, S. C. Polym Eng Sci 1995, 35, 1807.
20. Merfeld, G. D.; Pual, D. R. In Polymer Blends; Pual, D. R.; Bucknall, C. B., Eds.; Wiley: New York, 1999; Vol. 1, pp 1–81.
21. Stein, R. S.; Khambatta, F. B.; Warner, F. P.; Russell, T.; Escala, A.; Balizer, E. J Polym Sci Polym Symp 1978, 63, 313.
22. Yishikawa, K.; Molnar, A.; Eisenberg, A. Polym Eng Sci 1994, 34, 1056.